Control With Fault Detection Of The DC Microgrids Using SDRE-Controller-Observer

Linchao Ma[1*] and Jingkui Mao[2]

[1] School of Electrical Engineering and Automation, Henan Institute of Technology, Xinxiang, Henan 453003, China
[2] School of Electrical Engineering and Automation, Hefei University of Technology, Hefei, Anhui 230009, China
[*] Corresponding author. E-mail: Malinchao20@gmail.com

Received: Mar. 02, 2023; Accepted: July 28, 2023

In the present work, using the State-Dependent Riccati Equation approach, the optimal optimizer-controller is designed for a small DC network isolated from the network. The objectives are to control the output voltage of the solar cell, as well as output voltages of the battery, the capacitor bank and the DC busbar, and to detect possible faults in a timely manner. In the State-Dependent Riccati Equation observer–controller design process, a non-linear model is used for modeling the dynamic behavior of the microgrid in different operating conditions. The efficiency of the studied microgrid has been assessed in the presence of uncertainty in system parameters and measurement noise. The results of the simulations show the ability of the suggested approach to detect faults in a timely manner, not to recognize the disturbance as a fault, as well as the effective and resistant performance of the progressive controller even in the disturbance presence. Quantitatively, the proposed fault detection method was able to generate non-zero residual current in the presence of faults, allowing for fault detection by defining an appropriate threshold. The threshold used in the study was 50. Additionally, the fault detection system was able to avoid misdiagnosis of disturbances as faults.

Keywords: Micro grid, State-Dependent Riccati Equation, Fault Detection, DC network

http://dx.doi.org/10.6180/jase.202404_27(4).0003

1. Introduction

Due to declining fossil fuels and environmental issues, the renewable energy utilization in power systems is rapidly increasing. The availability of distributed generations in the system can affect the voltage and current of the network and have positive or negative impacts on the operating parameters of the system. Among the positive advantages of a microgrid, we can mention the increase of reliability, improvement of power quality, improvement of voltage profile, reduction of losses, etc. [1, 2].

A microgrid includes some distributed generations, an energy storing device, and loads, which can be operated as a network connection or island operation. In general, there are two kinds of microgrids, AC and DC, and DC microgrids have more advantages than AC microgrids. One example is the transfer of more power to a specific cable level [2]. In addition, there is no skin effect on DC microgrids, so the entire cable surface can be used to transmit current, which reduces losses in these DC microgrids. That's why in the same flow, DC microgrids require smaller cable diameters and less insulation.

Despite their advantages, microgrids still have problems during implementation, such as protecting and maintaining the internal stability of the microgrid in the presence of faults and changes in production capacity. DC rectifiers, which are used directly, are more challenging than AC microphones when detecting a fault. One of the reasons for this is the high transient current during the fault, the high cost of equipment to cut off this high current [3]. In recent studies, methods have been proposed to detect faults in DC microgrids. One of these methods is the use of differen-

tial protection, which depends on the connection between the two ends of the line [3, 4]. In this method, the voltage and current at the beginning and end of the line are measured and in case of a difference between the two, the system detects the fault and isolates the fault area. This approach has a main disadvantage that is the low reliability of the protection system. Another available protection is overcurrent protection. The function of this relay is such that a large current must pass through the system to the threshold of the relay excitation so that the relay detects a fault and issues a cut-off command. Going through such a large flow, even in the short term, can be problematic. Reference [2] suggests using a small processor relay to detect faults in low voltage networks. Finally, several methods of protection related to communication between the covered areas have been proposed for high-penetration distribution networks of wind turbines connected to the network [5, 6].

Observer-based techniques can be utilized to detect faults in microgrids in a codified manner. Reference [7] evaluates the use of a linear visor to protect the transmission line in an AC microgrid. Among the advantages and disadvantages of this approach are the rapid detection of fault and the invisibility of the observer against confusion. Reference [8] examines the use of linear visor to protect line and transformer using a minimum measurement sensor. Reference [9] has also used a nonlinear observer based on the State-Dependent Riccati Equation (SDRE) to detect faults in wind turbines. The results obtained from the references [9–11] indicate the capability for utilization of linear/nonlinear visual detectors for identification of faults in the microgrids. In these methods, the real output is compared to its nominal output, which is computed based on a mathematical model, and if there is a difference between the two, a non-zero residual current will be formed. Fault detection is possible.

The current SDRE equation design method was first proposed by Pearson in 1994 for approximation of the optimum control problem for non-linear models [12]. The presentation of non-linear systems as state-of-the-art linear systems named State-Dependent Coefficient (SDC) can be considered as the most important idea of this approach. There are various approaches based on quasi-linearization for solving different problems, like the design of a resistant H filter [12], the design of a sub-optimal sliding mode controller for systems with delay terms, and the design of a visor for a system. Rapid nonlinear lines [13], etc. are developed. Such approaches are applied positively for different applications. These approaches have some interesting features. For instance, the system efficiency can be affected by the designer in a predictable manner through setting weight functions [14]. As an example, increasing the weighted function of the system modes can accelerate the system response. This increment also will be resulted in growth of the control effort. Simultaneously, there is more degree of freedom for designer because of the impressive presence of SDC for the nonlinear system, which can be utilized for promotion of the total efficiency of the system used [15–18]. In addition, the SDRE approach maintains the nonlinear features of the system, which has high important from a practical view-point, especially for complex dynamics. A review of SDRE and related theories is reviewed in [12, 13]. However, the mentioned papers does not consider the integration of renewable energy sources and energy storage systems. Additionally, most of the papers does not provide a comparative analysis of the proposed method with other fault detection and control techniques for DC microgrids. Another limitation is that the proposed methods are based on a nonlinear model, which may increase the complexity of implementation and maintenance.

In this paper, considering the interesting properties of SDRE observers and controllers and the existence of nonlinear factors in the dynamics of DC microgrids, a new method for fault detection and control of these microgrids based on SDRE-nonlinear visor-controller is suggested. Be. Unlike the common protections mentioned above, adaptive protection systems are not required such as an overcurrent relay that must be adapted to network changes. This method has the appropriate speed and accuracy to detect faults and can detect small system faults and is resistant to clutter and noise. Hence, the contributions can be summarized as:

a) A new method for fault detection and control of DC microgrids based on SDRE-nonlinear visor-controller is suggested, which takes into account the non-linear factors in the dynamics of the microgrid.

b) The proposed method does not require adaptive protection systems such as an overcurrent relay that must be adapted to network changes, and has the appropriate speed and accuracy to detect faults, including small system faults.

c) This work describes the steps needed to design and develop the sustainability theories for the SDRE observer and controller. Other sections of this article are organized below: The second section introduces the system, containing the various sections of the microgrid, and the spatial model of its state. The third section is devoted to the study of the SDRE observer and controller and the steps needed to design and develop its sustainability theories. In fourth part, the results

of the simulation of the simulations conducted in the MATLAB environment are presented along with their analysis. Eventually, the fifth section is concluded the article.

2. Microgrid networks

Fig. 1 shows the structure of the DC microgrid, which is isolated from the main network. In this figure, the points where the fault occurred are identified. This microgrid consists of different equipment such as solar cell, battery, capacitor bank, and variable load. The management planning of desired microgrid is considered as follow: the production capacity of solar cells, which change alternately during the day, uses for supplying the variable load. If the Energy Storage Systems (ESSs) are empty, an amount of produced energy of the microgrid will be used to charge ESS. In contrast, if the production power of solar cell is less than the power consumption, ESSs will be discharged and the voltage of microgrid will be fixed.

It should be noted that in the microgrid of Fig. 1, the capacitor of C_9 is used to reduce the ripple of output voltage. In the following, descriptions of various sections of DC microgrid are given, and the mathematical model of the studied microgrid is studied.

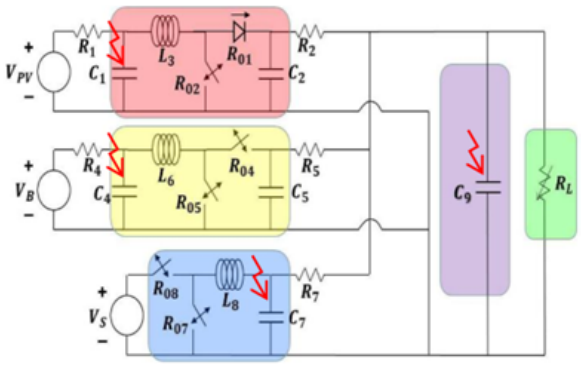

Fig. 1. The studied microgrid

2.1. Solar Cell

Regarding Fig. 1, the solar cell is linked to the DC busbar using a DC-DC converter. The measured variables are as I_{L3}, V_{C1}, and V_{C2} that represent the current of inductor L_3, the voltage of capacitor C_1, and voltage of capacitor C_2, respectively. Input control as $0 \leq u_1 \leq 1$ is considered as the duty cycle of converter.

2.2. Battery

As depicted in Fig. 1, the battery is also linked to the microgrid busbar by a DC-DC converter. In this model, the measured variables are as I_{L6}, V_{C4}, and V_{C5}, which indicate the current of inductor L_6, the voltage of capacitor C_4, and voltage of capacitor C_5, respectively. In addition, the input control of $0 \leq u_2 \leq 1$ is considered as the duty cycle of its converter.

2.3. Capacitor Bank

In Fig. 1, the capacitor bank by DC-DC converter is connected to the microgrid busbar. In the model of capacitor bank, the measured variables are as I_{L8} and V_{C7}, which show the current of inductor L_8 and voltage of capacitor C_7, respectively. In addition, the input control of $0 \leq u_3 \leq 1$ is considered as the duty cycle of converter.

2.4. The Model of Studied Microgrid

The state variables could be defined as follows:

$$\begin{aligned} x_1 &= V_{c1} \\ x_2 &= V_{c2} \\ x_3 &= V_{c3} \\ x_4 &= V_{c4} \\ x_5 &= V_{c5} \\ x_6 &= V_{c6} \\ x_7 &= V_{c7} \\ x_8 &= V_{c8} \\ x_9 &= V_{c9} \end{aligned} \tag{1}$$

Then, the model of the studied microgrid could be considered as follow:

$$\begin{aligned} \dot{x_1} &= -\frac{1}{R_1 \cdot C_1} \cdot x_1 - \frac{1}{C_1} \cdot x_3 + \frac{1}{R_1 \cdot C_1} \cdot V_{PV} \\ \dot{x_2} &= -\frac{1}{R_2 \cdot C_2} \cdot x_2 + \frac{1}{C_2} \cdot x_3 - \frac{1}{C_2} \cdot u_1 \cdot x_3 + \frac{1}{R_2 \cdot C_2} \cdot x_9 \\ \dot{x_3} &= \frac{1}{L_3} [x_1 - x_2 - R_{01} x_3] + \frac{1}{L_3} [x_2 + R_{01} - R_{02}] \cdot u_1 \\ \dot{x_4} &= -\frac{1}{R_4 \cdot C_4} \cdot x_4 - \frac{1}{C_4} \cdot x_6 + \frac{1}{R_4 \cdot C_4} \cdot V_B \\ \dot{x_5} &= -\frac{1}{R_5 \cdot C_5} \cdot x_5 - \frac{1}{C_5} \cdot x_6 - \frac{1}{C_5} \cdot u_2 \cdot x_5 + \frac{1}{R_5 \cdot C_5} \cdot x_9 \\ \dot{x_6} &= \frac{1}{L_6} [x_4 - x_5 - R_{04} x_6 + u_2 \cdot x_5] \\ \dot{x_7} &= -\frac{1}{R_7 \cdot C_7} \cdot x_7 - \frac{1}{C_7} \cdot x_8 + \frac{1}{R_7 \cdot C_7} \cdot x_9 \\ \dot{x_8} &= \frac{1}{L_8} [u_3 \cdot V_S - x_7 - R_{08} x_8] \\ \dot{x_9} &= \frac{1}{C_9} \left[\frac{x_2 - x_9}{R_2} + \frac{x_5 - x_9}{R_5} + \frac{x_7 - x_9}{R_7} - \frac{x_9}{R_L} \right] \end{aligned} \tag{2}$$

The parameters of model in Eq. (2) are given in Table 1 [20]. It should be noted that the above equation represents a non-linear system due to the presence of multiplicative factors of $u_1 \cdot x_3$, $u_2.x_2$, and $u_2.x_5$.

Table 1. The value of the parameters of the studied microgrid

Parameters	Value	Parameters	Value (Ω)
C_1	0.1000(F)	R_1	0.1000
C_2	0.0100(F)	R_2	0.1000
C_4	0.1000(F)	R_4	0.1000
C_5	0.0100(F)	R_5	0.0100
C_7	0.0100(F)	R_7	0.1000
C_9	0.0001(F)	R_{01}	0.0100
		R_{02}	0.0100
L_3	0.0330(H)	R_{04}	0.0100
L_6	0.0330(H)	R_{05}	0.0100
L_8	0.0033(H)	R_{07}	0.0100
		R_{08}	0.0100
$V_{bus.}$	1000.0(V)		

3. Non-linear SDRE sub-optimal controller-observer

In this section, the process of designing of a SDRE controller and non-linear observer is presented.

3.1. SDRE Controller

Consider the below non-linear system:

$$\dot{x}(t) = f(x(t)) + B \cdot u(t), x(t=0) = x_0 \tag{3}$$

In which, $x(t). \in \Re^n$ and $u(t), \in \Re^m$ denote the state and input control vectors, and x_0 is the value of the initial condition. Presentation of the nonlinear model in a quasi-linear form is the main idea of the SDRE approach [3]. In this way, a factorization is done as follow:

$$f(x(t)) = A(x(t)) \cdot x(t) \tag{4}$$

Where, $A(x(t)) \in \Re^n \rightarrow \Re^{n \times n}$ is considered as the matrix depended to the state. The main point of this factorization is the existence of countless possibilities for the decomposition of $f(x(t))$ as a coefficient of $x(t)$. As an instance, if the functions $f(x(t)) = A_1(x(t)) \cdot x(t)$ and $f(x(t)) = A_2(x(t)) \cdot x(t)$ considered for $f(x(t))$, all other linear combinations of $A_1(x(t))$ and $A_2(x(t))$ could be another quasi-linear construction as follow, which $a(x(t))$ is a known function of $x(t)$:

$$A(x(t)) = a(x(t)) \cdot A_1(x(t)) + (1 - a(x(t)) \cdot A_2(x(t))) \tag{5}$$

This can be considered as an advantage of the SDRE approach, which gives more freedom to designer. One of the main targets in optimal stabilizer is to obtain a pattern that can be used for bringing the system status to the desired equilibrium point as well as the predefined cost function will be minimized. In the SDRE, the cost function is considered as follow [9]:

$$J = \frac{1}{2} \int_0^\infty \left[x^T(t) \cdot Q(x(t)) \cdot x(t) + u^T(t) \cdot R(x(t)) \cdot u(t) \right] dt \tag{6}$$

In which, $R(x(t))$ and $Q(x(t))$ are the weighted matrices that depend to the state, and are in the form of a definite positive pointed and a semi-definite positive pointed, respectively. The presented optimization problem in Eq. (3) and Eq. (6) will be solved to obtain the solution of the Hamilton-Jacobi-Bellman (HJB) relation. Furthermore, this HJB equation has high complexity generally. In SDRE approach, it's depicted that control pattern as Eq. (7) can be utilized for finding an approximate solution to the mentioned problem:

$$u(t) = -R^{-1}(x(t)) \cdot B^T(x(t)) \cdot P(x(t)) \cdot x(t) \tag{7}$$

In which, the $P(x(t))$ is the definite positive solution of the equation that is depended to follow state:

$$\begin{aligned} &A^T x(t) \cdot P(x(t)) + P(x(t)) \cdot A(x(t)) - \cdots \\ &\cdots P(x(t)) \cdot B(x(t)) \cdot R^{-1} x(t) \cdot B^T x(t) \cdot P(x(t)) + Q(x(t)) \\ &= 0 \end{aligned} \tag{8}$$

It's remarkable that Eq. (8) has a symmetric positive uniformity solution only if the pairs $\{A(x(t)), B(x(t))\}$ and $\left\{A(x(t)), Q^{1/2}(x(t))\right\}$ be the point-to-point sustainable and detectable, respectively [9]. The authors of [9] verified that equilibrium at the origin of the closed-loop model resulting from the SDRE controller is locally stable. Although there are various methods for selection of matrix $A(x(t))$, only one of the many possible SDC leads to optimum efficiency of the closed-loop model. However, the finding of this optimized SDC is so difficult. So, the aim constraint to choose $A(x(t))$ should be satisfied in Eq. (4).

3.2. SDRE Observer

Let to assume the below non-linear system:

$$\dot{x} = f(x), y = h(x) \tag{9}$$

In which, $x \in \Re^n$ and $y \in \Re^m$ are the state and output vectors. The purpose of the control problem is to find the estimation of the state vector, i.e. x matrix. In this paper, we supposed the $\dot{x}$ as the estimated vector of x. According

to the first theorem of [15], the fault estimation of the SDRE observer, as $e = x - \dot{x}$, will be tended to zero with an asymptote line. In essence, the SDRE observer construction could be considered in the following form:

$$\begin{cases} \dot{\hat{x}} = A(\hat{x}) \cdot \hat{x} + L(\hat{x}) \cdot [y - C(\hat{x}) \cdot \hat{x}] \\ f(\hat{x}) = A(\hat{x}) \cdot \hat{x} \\ h(\hat{x}) = C(\hat{x}) \cdot \hat{x} \end{cases} \quad (10)$$

Where, $L(\hat{x})$ is the observer gain, which could be obtained as follow:

$$L(\hat{x}) = P(\hat{x}) \cdot C^T \cdot \hat{x}(t) \cdot V^{-1} \quad (11)$$

In Eq. (10), $S(\hat{x})$ is considered as the solution of the Riccati Equation (RE) that is as follow:

$$A(\hat{x}) \cdot S(\hat{x}) + S(\hat{x}) \cdot A^T(\hat{x}) - S(\hat{x}) \cdot C^T(\hat{x}) \cdot V^{-1} + C(\hat{x}) \cdot S(\hat{x}) + W = 0 \quad (12)$$

According to the first theorem in [14], for achieving a stable SDRE observer, it's essential for the pair $(A^T(\hat{x}), C^T(\hat{x}))$ to be stable for all values of $\hat{x} \in \Re^n$. Moreover, the weighted matrices of $V \in \Re^{P \times P}$ and $W \in \Re^{n \times n}$ are symmetrical that are determined by the designer. It's worthy to note that V and W are semi-definite and definite positives, respectively. In addition, the stability of the observer means that the fault estimate $e(t)$ is tended to zero with an asymptote line.

4. Simulation results

Obtained results in this section are separated into two sections. The first section deals with the controlling of the output voltage of the solar cell, battery, capacitor bank and DC busbar considering parameter uncertainties and SDRE controller. The second section is devoted to the analysis of the results of applying the SDRE observer for in-time faults detection.

4.1. SDRE Control

The control aims in the studied microgrid are to regulate the output voltages of the solar cell, battery and DC busbar, which can be achieved using inputs of $u_1(t)$, $u_2(t)$, and $u_3(t)$. For this purpose, in the first step, the desired equilibrium point of the system could be obtained by equaling the right side of Eq. (2) to zero. Therefore, there are 9 equations with 12 variables.

With considering the optimal values of the output voltages of the solar cell, the battery, and the DC busbar as 300 V, 400 V, and 1000 V, respectively, there will be 9 equations with 9 variables. It is necessary to mention that according to the right side of Eq. (2), solving of the multi-equations will be simple.

In other words, there will be 3 equations with 3 variables. For the variables of the studied microgrid, the equilibrium is obtained as tabulated in Table 2. By defining the new variables as $\Delta x_i = x_i - x_i^*$ that $i = \{1,2,3,\ldots,9\}$, and $\Delta u_i = u_i - u_i^*$ that $i = \{1,2,3\}$, as well as according to (2), the space model of the following state can be obtained that its equilibrium is achieved in the origin:

$$\begin{aligned}
\Delta\dot{x}_1 &= -\frac{1}{R_1 \cdot C_1} \cdot \Delta x_1 - \frac{1}{C_1} \cdot \Delta x_3 \\
\Delta\dot{x}_2 &= -\frac{1}{R_2 \cdot C_2} \cdot \Delta x_2 + \frac{0.3}{C_2} \cdot \Delta x_3 - \frac{1}{C_2} \cdot \Delta u_1 \cdot \Delta x_3 + \frac{1}{R_2 \cdot C_2} \cdot \Delta x_9 \\
\Delta\dot{x}_3 &= \frac{1}{L_3} [\Delta x_1 - 0.3\Delta x_2 - R_{01}\Delta x_3] + \frac{1}{L_3}\Delta x_2 \cdot \Delta u_1 \\
\Delta\dot{x}_4 &= -\frac{1}{R_4 \cdot C_4} \cdot \Delta x_4 - \frac{1}{C_4} \cdot \Delta x_6 \\
\Delta\dot{x}_5 &= -\frac{1}{R_5 \cdot C_5} \cdot \Delta x_5 - \frac{0.004}{C_5} \cdot \Delta x_6 \mp \frac{1}{C_5} \cdot \Delta u_2 \cdot \Delta x_5 + \frac{1}{R_5 \cdot C_5} \cdot \Delta x_9 \\
\Delta\dot{x}_6 &= \frac{1}{L_6} [\Delta x_4 - 0.4\Delta x_5 - R_{04}\Delta x_6 + \Delta u_2 \cdot \Delta x_5] \\
\Delta\dot{x}_7 &= -\frac{1}{R_7 \cdot C_7} \cdot \Delta x_7 + \frac{1}{C_7} \cdot \Delta x_8 + \frac{1}{R_7 \cdot C_7} \cdot \Delta x_9 \\
\Delta\dot{x}_8 &= \frac{1}{L_8} [\Delta u_3 . V_S - \Delta x_7 - R_{08}\Delta x_8] \\
\Delta\dot{x}_9 &= \frac{1}{C_9} \left[\frac{\Delta x_2 - \Delta x_9}{R_2} + \frac{\Delta x_5 - \Delta x_9}{R_5} + \frac{\Delta x_7 - \Delta x_9}{R_7} - \frac{\Delta x_9}{R_L} \right]
\end{aligned} \quad (13)$$

For designing the SDRE controller and observer, it's essential to consider an SDC display from system (13). Due to this system has 9 state variables, there are countless of SDC for it. In our simulations, the SDC is utilized with the matrices A and $B(x(t))$ as follows:

$$A = \begin{bmatrix}
-\frac{1}{R_1 \cdot C_1} & 0 & -\frac{1}{C_1} & 0 & 0 & 0 & 0 & 0 & 0 \\
0 & -\frac{1}{R_2 \cdot C_2} & \frac{0.3}{R_2 \cdot C_2} & 0 & 0 & 0 & 0 & 0 & \frac{1}{R_2 \cdot C_2} \\
\frac{1}{L_3} & -\frac{0.3}{L_3} & -\frac{0.01}{L_6} & 0 & 0 & 0 & 0 & 0 & 0 \\
0 & 0 & 0 & -\frac{1}{R_4 \cdot C_4} & 0 & -\frac{1}{C_4} & 0 & 0 & 0 \\
0 & 0 & 0 & 0 & -\frac{1}{R_5 \cdot C_5} & \frac{0.004}{R_5 \cdot C_5} & 0 & 0 & -\frac{1}{R_5 \cdot C_5} \\
0 & 0 & 0 & \frac{1}{L_6} & -\frac{0.4}{L_6} & -\frac{0.01}{L_6} & 0 & 0 & 0 \\
0 & 0 & 0 & 0 & 0 & 0 & -\frac{1}{R_7 \cdot C_7} & \frac{1}{C_7} & \frac{1}{R_7 \cdot C_7} \\
0 & 0 & 0 & 0 & 0 & 0 & -\frac{1}{L_8} & -\frac{R_{08}}{L_8} & 0 \\
0 & -\frac{1}{R_2 \cdot C_9} & 0 & 0 & -\frac{1}{R_5 \cdot C_9} & 0 & -\frac{1}{R_7 \cdot C_9} & 0 & -\frac{1}{C_9}\left[\frac{1}{R_2} + \frac{1}{R_5} + \frac{1}{R_7} - \frac{1}{R_L}\right]
\end{bmatrix} \quad (14)$$

$$B(x(t)) = \begin{bmatrix} 0 & -\frac{x_3}{C_2} & \frac{x_2+1000}{L_9} & 0 & 0 & 0 & 0 & 0 & 0 \\ 0 & 0 & 0 & 0 & -\frac{x_6}{C_5} & \frac{x_5+1000}{L_6} & 0 & 0 & 0 \\ 0 & 0 & 0 & 0 & 0 & 0 & 0 & \frac{1900}{L_8} & 0 \end{bmatrix}$$

The selected weighted matrices are selected as follows in the simulations performed. In the selection of these weight matrices, the method presented in [19] has been used.

Table 2. The optimal value of system variables

Variables	Value	Variables	Value
x_1^*	300.0	x_7^*	1000
x_2^*	1000	x_8^*	5.000
x_3^*	0.000	x_9^*	1000
x_4^*	400.0	u_1^*	0.700
x_5^*	1000	u_2^*	0.600
x_6^*	0.000	u_3^*	0.500

$$Q = 10I_9 \& R = 10^{-6}\,\mathrm{diag}(0.009, 7, 2) \tag{15}$$

In the simulation process, it's considered that the studied microgrid is exposed to different disturbances such as solar cell voltage (V_{p_v}), the battery voltage (V_B), capacitor bank voltage (V_S), load changes, and applied noise into microgrid. It's remarkable that it's considered here, mentioned disturbances change independently. Curves of these disturbances are depicted in Fig. 2 and Fig. 3.

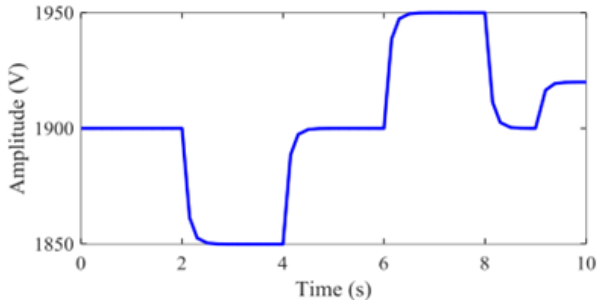

Fig. 2. The variations of the capacitor bank voltage

The results of the performed simulations with SDRE controller are depicted in Fig. 4. As shown in this figure, despite the drastic changes in voltage of capacitors C_1 and C_4, the SDRE controller has ability for maintaining the system stability.

With the simultaneous applied disturbances of R_L, V_S, V_B, and V_{pp} in the presence of the controller SDRE, the voltage variations of solar cell and battery is shown in Fig. 5. In addition, their currents are shown in Fig. 6, in the same condition. As shown in both figures, after a few

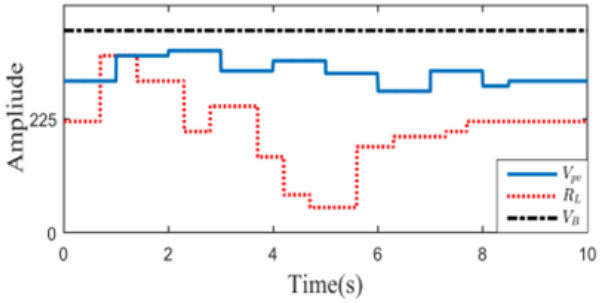

Fig. 3. The voltage variations of the solar cell, the battery, and load

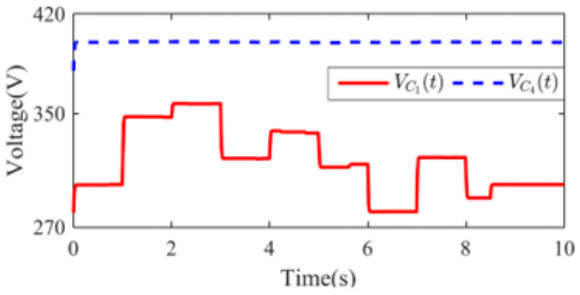

Fig. 4. The voltage variations of the capacitors C_1 and C_4 in the presence of SDRE

seconds, the voltages and currents could be controlled and restores to the balance conditions.

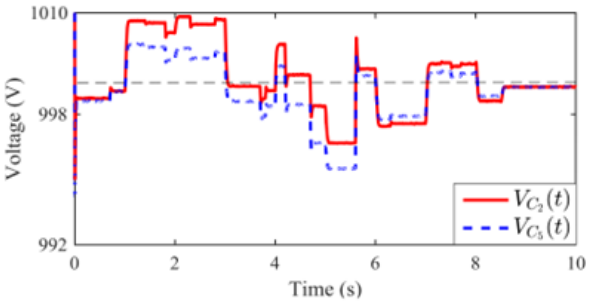

Fig. 5. The voltage variations of the solar cell and the battery in the presence of SDRE

The variations of voltage of the capacitor bank and its current considering the output power and load disturbances are plotted in Fig. 7 and Fig. 8, respectively. As seen in these figures, despite the important disturbances, the suggested method has modified and optimized the voltage and current. Therefore, the equilibrium points after a few seconds have been obtained and the system stability has been maintained.

Fig. 9 shows the voltage of the capacitor C_9 of the DC busbar, which is used to establish the steady state condi-

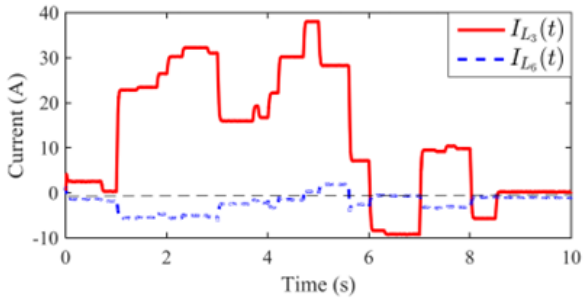

Fig. 6. The current variations of the solar cell and the battery in the presence of SDRE

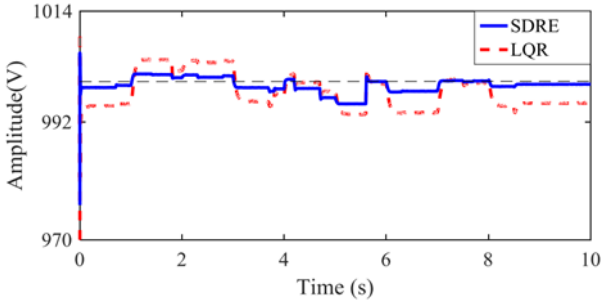

Fig. 9. The voltage variations of the DC busbar in the presence of SDRE

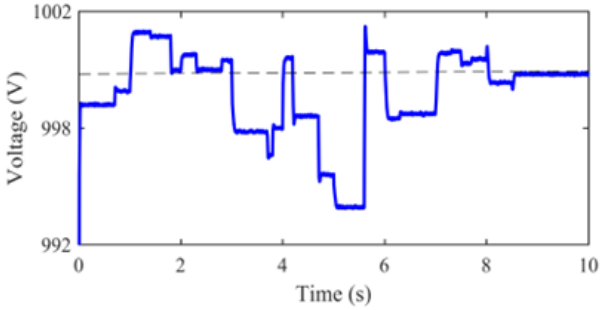

Fig. 7. The voltage variations of the capacitor bank with SDRE

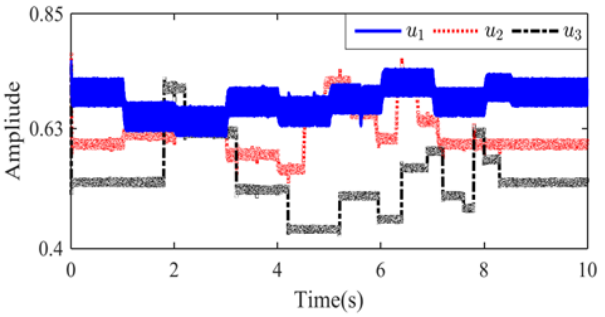

Fig. 10. The applied signals on the power system

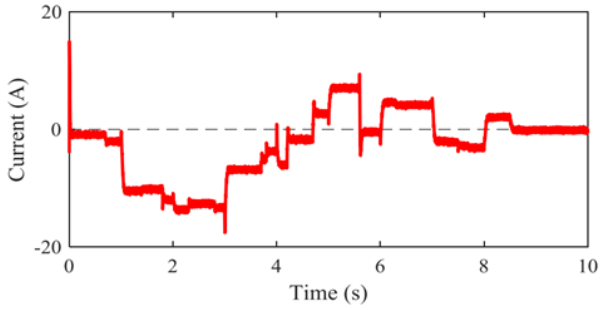

Fig. 8. The current variations of the capacitor bank with SDRE

tions during load changes as well as output power variations. As seen in this figure, under the applied disturbances and noise to the microgrid, the SDRE controller has been able to control the voltage well and ensure the system stability.

Fig. 10 shows the applied signals to the studied system. As shown in this figure, the amplitude of the input control is small despite the drastic changes of the output voltages of the solar cell, the capacitive bank, the value of load, as well as the applied noise to all measurement variables. Therefore, the obtained results indicate that the suggested approach can be conquered the disturbed systems.

4.2. Control with Fault Diagnosis Based on SDRE

The performance of the SDRE-based fault detection system are studied here. For this purpose, the SDC configuration of the result of Eq. (13) is used. The weighted matrices of W and V are regarded as:

$$V = 10^{-4} I_9 \quad \& W = 10^6 \,\mathrm{diag}(1, 50, 1, 1, 50, 1, 50) \qquad (16)$$

It's considered that a fault occurred at 1.5 ms in capacitor C_1 and another fault occurred in capacitor C_4 at 3.5 ms. The results of the mentioned conditions are illustrated in Figs. 11 and 12. As seen in Fig. 11, the voltage of capacitor C_1 has dropped from 300 V to 10 V and the voltage of capacitor C_4 has dropped from 400 V to 10 V. Corresponding to the decreased voltages, as seen in Fig. 12, the output current of the solar cell and the battery were reduced.

Meanwhile, the fault identification method by comparing the real output of the system with the SDRE observer's output has formed a non-zero residual current according to Fig. 13, which the fault detection is possible by defining the appropriate threshold (here we have assumed a threshold of 50). As mentioned before, a significant issue in the fault detection is the lack of misdiagnosis of confusion as fault. As mentioned priorly, despite the mentioned disturbances, it's depicted in Fig. 12 that the fault alarm system is not

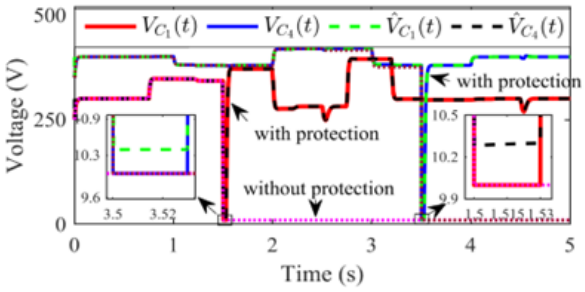

Fig. 11. The voltages variations of the capacitors C_1 and C_4 under the fault conditions

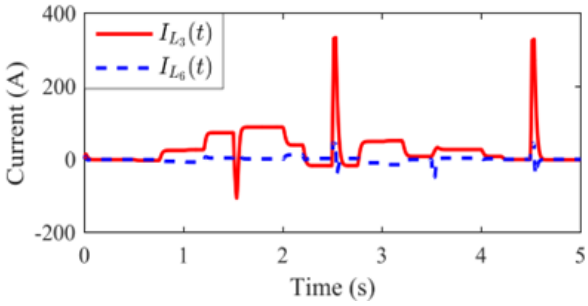

Fig. 12. The currents variations of the inductors L_3 and L_6 under the fault conditions

activated at these times.

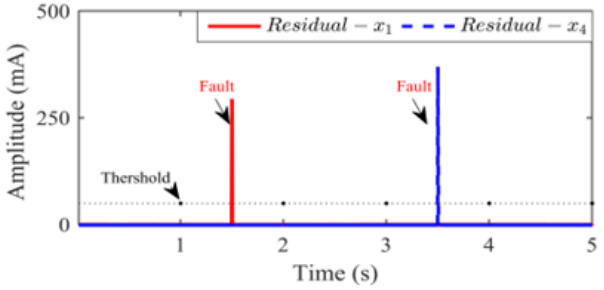

Fig. 13. The residual currents variations of the capacitors C_1 and C_4 under the fault conditions

For depicting the capability of the fault detection and control system and its nondependence on the fault location, a fault applied on the output of capacitor C_7 at 2.5 ms, and another fault occurred on the busbar at 4.5 ms. The results of these conditions are shown in Fig. 14 and Fig. 15. As shown in these figures, at 2.5 ms, the voltage of capacitor C_7 has dropped from 1000 V to 500 V, and the busbar voltage has dropped from 1000 volts to 500 volts. In this case, as can be seen from Fig. 16, the output current of the capacitor bank has increased. Fig. 17 illustrates that it is possible for identification of the faults by considering an appropriate threshold level for fault detection.

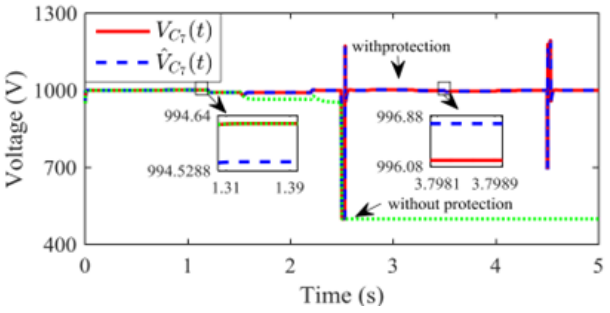

Fig. 14. The output voltage variations of the capacitor bank, under the fault on the capacitor C_7

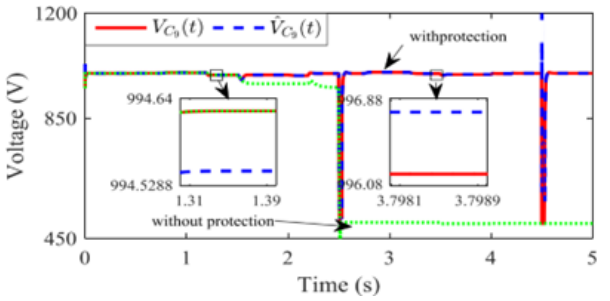

Fig. 15. The output voltage variations of the busbar, under the fault on the capacitor C_8

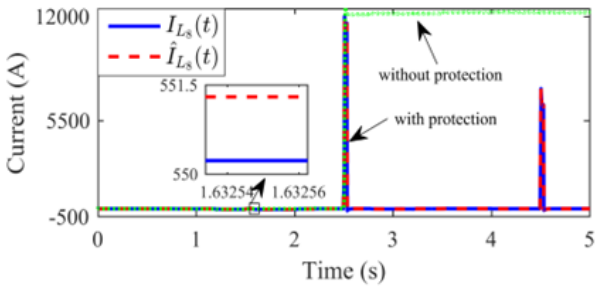

Fig. 16. The output current variations of the capacitor bank

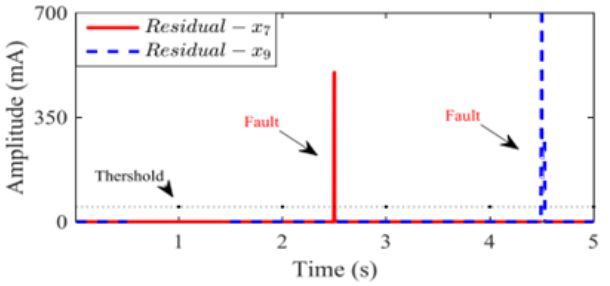

Fig. 17. The residual currents variations of the capacitors C_7 and C_9 under the fault conditions

Accordingly, Figs. 11 and 12 illustrate the effect of two different faults on the voltage and current of the system.

Fig. 11 shows the voltage drop in capacitors C1 and C4, which results in reduced output current of the solar cell and battery. Fig. 12 demonstrates that the fault detection system is able to detect the faults without triggering false alarms.

Fig. 13 presents the non-zero residual current resulting from the fault identification method using the SDRE observer's output, indicating the possibility of fault detection by defining an appropriate threshold.

Figs. 14 and 15 show the effect of two different faults on the voltage of capacitor C7 and the busbar, respectively. Fig. 16 demonstrates the increase in the output current of the capacitor bank due to the fault, and Fig. 17 shows the possibility of fault identification by setting an appropriate threshold level for fault detection. These figures demonstrate the capability of the fault detection and control system and its non-dependence on the fault location.

5. Conclusion

The proposed fault detection approach based on the SDRE observer offers a fast and reliable method for protecting DC microgrids. By comparing the system's real output with the nominal output computed through a nonlinear observer, faults can be quickly detected without the risk of misdiagnosis. The approach also offers the advantage of being able to maintain microgrid efficiency in the presence of external disturbances and measurement noise. Furthermore, the use of an SDRE controller allows for adjustment of the system's output voltage, with simulation results demonstrating the controller's effectiveness in achieving its intended goals. However, it is important to note that the limitations of the study, such as the lack of consideration for renewable energy sources and energy storage systems and the absence of comparative analysis with other techniques, should also be taken into account. Future research should aim to address these limitations to further improve the proposed approach. As a future work, we can consider some more points a:

- Comparative analysis: While the proposed approach demonstrated promising results, future research could compare the performance of the SDRE observer-based approach with other fault detection techniques to determine its effectiveness and superiority.
- Real-world implementation: The proposed approach has only been tested through simulations. Future research could focus on implementing the approach in a real-world microgrid to validate its effectiveness and practicality.

References

[1] S. Huang and O. Abedinia, (2021) *"Investigation in economic analysis of microgrids based on renewable energy uncertainty and demand response in the electricity market"* **Energy *225***: 120247. DOI: https://doi.org/10.1016/j.energy.2021.120247.

[2] C. Wang, Z. Zhang, O. Abedinia, and S. G. Farkoush, (2021) *"Modeling and analysis of a microgrid considering the uncertainty in renewable energy resources, energy storage systems and demand management in electrical retail market"* **Journal of Energy Storage *33***: 102111. DOI: https://doi.org/10.1016/j.est.2020.102111.

[3] J.-D. Park and J. Candelaria, (2013) *"Fault Detection and Isolation in Low-Voltage DC-Bus Microgrid System"* **IEEE Transactions on Power Delivery *28***(2): 779–787. DOI: 10.1109/TPWRD.2013.2243478.

[4] J.-D. Park, J. Candelaria, L. Ma, and K. Dunn, (2013) *"DC Ring-Bus Microgrid Fault Protection and Identification of Fault Location"* **IEEE Transactions on Power Delivery *28***(4): 2574–2584. DOI: 10.1109/TPWRD.2013.2267750.

[5] G. P. Adam, F. Alsokhiry, and A. Alabdulwahab, (2022) *"DC grid controller for optimized operation of voltage source converter based multi-terminal HVDC networks"* **Electric Power Systems Research *202***: 107595. DOI: https://doi.org/10.1016/j.epsr.2021.107595.

[6] A. Ahl, M. Yarime, M. Goto, S. S. Chopra, N. M. Kumar, K. Tanaka, and D. Sagawa, (2020) *"Exploring blockchain for the energy transition: Opportunities and challenges based on a case study in Japan"* **Renewable and Sustainable Energy Reviews *117***: 109488. DOI: https://doi.org/10.1016/j.rser.2019.109488.

[7] M. A. Zamani, T. S. Sidhu, and A. Yazdani, (2011) *"A Protection Strategy and Microprocessor-Based Relay for Low-Voltage Microgrids"* **IEEE Transactions on Power Delivery *26***(3): 1873–1883. DOI: 10.1109/TPWRD.2011.2120628.

[8] S. Matos, M. Vargas, L. Fracalossi, L. Encarnação, and O. Batista, (2021) *"Protection philosophy for distribution grids with high penetration of distributed generation"* **Electric Power Systems Research *196***: 107203. DOI: https://doi.org/10.1016/j.epsr.2021.107203.

[9] A. Hwas and R. Katebi. "Nonlinear observer-based fault detection and isolation for wind turbines". In: *22nd Mediterranean Conference on Control and Automation*. 2014, 870–875. DOI: 10.1109/MED.2014.6961483.

[10] M. Esreraig and J. Mitra. "An observer-based protection system for microgrids". In: *2011 IEEE Power and Energy Society General Meeting*. 2011, 1–7. DOI: 10.1109/PES.2011.6039818.

[11] M. Esreraig and J. Mitra, (2015) *"Microgrid protection using system observer and minimum measurement set"* **International Transactions on Electrical Energy Systems *25***(4): 607–622. DOI: https://doi.org/10.1002/etep.1849. eprint: https://onlinelibrary.wiley.com/doi/pdf/10.1002/etep.1849.

[12] T. Çimen, (2010) *"Systematic and effective design of nonlinear feedback controllers via the state-dependent Riccati equation (SDRE) method"* **Annual Reviews in Control *34***(1): 32–51. DOI: https://doi.org/10.1016/j.arcontrol.2010.03.001.

[13] T. Çimen, (2012) *"Survey of State-Dependent Riccati Equation in Nonlinear Optimal Feedback Control Synthesis"* **Journal of Guidance, Control, and Dynamics *35***(4): 1025–1047. DOI: 10.2514/1.55821.

[14] T. T. Darabseh, (2022) *"Nonlinear State Dependent Riccati Equation Controller for 3-DOF Airfoil with Cubic Structural Nonlinearity"* **International Review of Aerospace Engineering *15***(2): 97–111. DOI: 10.15866/irease.v15i2.21426.

[15] Y. Batmani and H. Khaloozadeh, (2016) *"On the design of suboptimal sliding manifold for a class of nonlinear uncertain time-delay systems"* **International Journal of Systems Science *47***(11): 2543–2552. DOI: 10.1080/00207721.2014.999263.

[16] Y. Batmani and H. Khaloozadeh, (2014) *"On the design of observer for nonlinear time-delay systems"* **Asian Journal of Control *16***(4): 1191–1201. DOI: 10.1002/asjc.795.

[17] Y. Batmani and H. Khaloozadeh, *"Optimal chemotherapy in cancer treatment: state dependent Riccati equation control and extended Kalman filter"* **Optimal Control Applications and Methods *34***(5): 562–577. DOI: https://doi.org/10.1002/oca.2039. eprint: https://onlinelibrary.wiley.com/doi/pdf/10.1002/oca.2039.

[18] T. D. Do, H. H. Choi, and J.-W. Jung, (2012) *"SDRE-Based Near Optimal Control System Design for PM Synchronous Motor"* **IEEE Transactions on Industrial Electronics *59***(11): 4063–4074. DOI: 10.1109/TIE.2011.2174540.

[19] Y. Batmani, M. Davoodi, and N. Meskin, (2017) *"Nonlinear Suboptimal Tracking Controller Design Using State-Dependent Riccati Equation Technique"* **IEEE Transactions on Control Systems Technology *25***(5): 1833–1839. DOI: 10.1109/TCST.2016.2617285.